LETTER • OPEN ACCESS

Untangling the impacts of socioeconomic and climatic changes on vegetation greenness and productivity in Kazakhstan

View the article online for updates and enhancements.

You may also like

ENVIRONMENTAL RESEARCH
LETTERS

LETTER

Untangling the impacts of socioeconomic and climatic changes on vegetation greenness and productivity in Kazakhstan

Kolluru Venkatesh[1,*] , Ranjeet John[1,2] , Jiquan Chen[3,4] , Meghann Jarchow[1], Reza Goljani Amirkhiz[2], Vincenzo Giannico[5] , Sakshi Saraf[2] , Khushboo Jain[1], Maira Kussainova[6,7] and Jing Yuan[4]

1 Department of Sustainability and Environment, University of South Dakota, Vermillion, SD 57069, United States of America
2 Department of Biology, University of South Dakota, Vermillion, SD 57069, United States of America
3 Department of Geography, Environment, and Spatial Sciences, Michigan State University, East Lansing, MI 48823, United States of America
4 Center for Global Change and Earth Observations, Michigan State University, East Lansing, MI 48823, United States of America
5 Department of Agricultural and Environmental Sciences, University of Bari A. Moro, Via Amendola 165/A, 70126 Bari, Italy
6 Kazakh National Agrarian Research University, AgriTech Hub KazNARU, 8 Abay Avenue, Almaty 050010, Kazakhstan
7 Kazakh-German University (DKU), 173 Nazarbaev Avenue, Almaty 050010, Kazakhstan
* Author to whom any correspondence should be addressed.

E-mail: Venkatesh.Kolluru@coyotes.usd.edu

Abstract

Studies examining the joint interactions and impacts of social-environmental system (SES) drivers on vegetation dynamics in Central Asia are scarce. We investigated seasonal trends and anomalies in drivers and their impacts on ecosystem structure and function (ESF). We explored the response of net primary production, evapotranspiration and normalized difference vegetation index (NDVI) to various SES drivers—climate, human influence, heat stress, water storage, and water content—and their latent relationships in Kazakhstan. We employed 13 predictor drivers from 2000 to 2016 to identify the interactions and impacts on ESF variables that reflect vegetation growth and productivity. We developed 12 models with different predictor–response variable combinations and separated them into two approaches. First, we considered the winter percent snow cover (SNOWc) and spring rainfall (P_MAM) as drivers and then as moderators in a structural equation model (SEM). SNOWc variability (SNOWc$_{SD}$) as an SEM moderator exhibited superior model accuracy and explained the interactions between various predictor–response combinations. Winter SNOWc$_{SD}$ did not have a strong direct positive influence on summer vegetation growth and productivity; however, it was an important moderator between human influence and the ESF variables. Spring rainfall had a stronger impact on ESF variability than summer rainfall. We also found strong positive feedback between soil moisture (SM) and NDVI, as well as a strong positive influence of vegetation optical depth (VOD) and terrestrial water storage (TWS) on ESF. Livestock density (LSK$_D$) exhibited a strong negative influence on ESF. Our results also showed a strong positive influence of socioeconomic drivers, including crop yield per hectare (CROPh), gross domestic product per capita (GDPca), and population density (POP$_D$) on vegetation productivity. Finally, we found that vegetation dynamics were more sensitive to SM, VOD, LSK$_D$ and POP$_D$ than climatic drivers, suggesting that water content and human influence drivers were more critical in Kazakhstan.

1. Introduction

Asian drylands, which account for 30% of global drylands, are in developing countries where livelihoods rely on land and ecosystem services. These countries have experienced socio-ecological, environmental, and institutional shifts causing grassland degradation, livestock mortality and conflicts over water

resources (Gutman *et al* 2020, Chen *et al* 2022). Rapid population growth and ongoing climate change in these drylands are causing additional pressure on these fragile grassland ecosystems (Hao *et al* 2018). Consequently, Asian drylands are identified as land-use and climate change hotspots that are vulnerable to ecological and environmental degradation (de Beurs *et al* 2018). However, little is known about long-term vegetation changes, grassland degradation and drivers associated with human-environmental interactions (Abel *et al* 2021, Venkatesh *et al* 2022). Investigating vegetation dynamics and the underlying drivers is crucial for preventing further degradation and restoring degraded grassland ecosystems (Meyfroidt *et al* 2016).
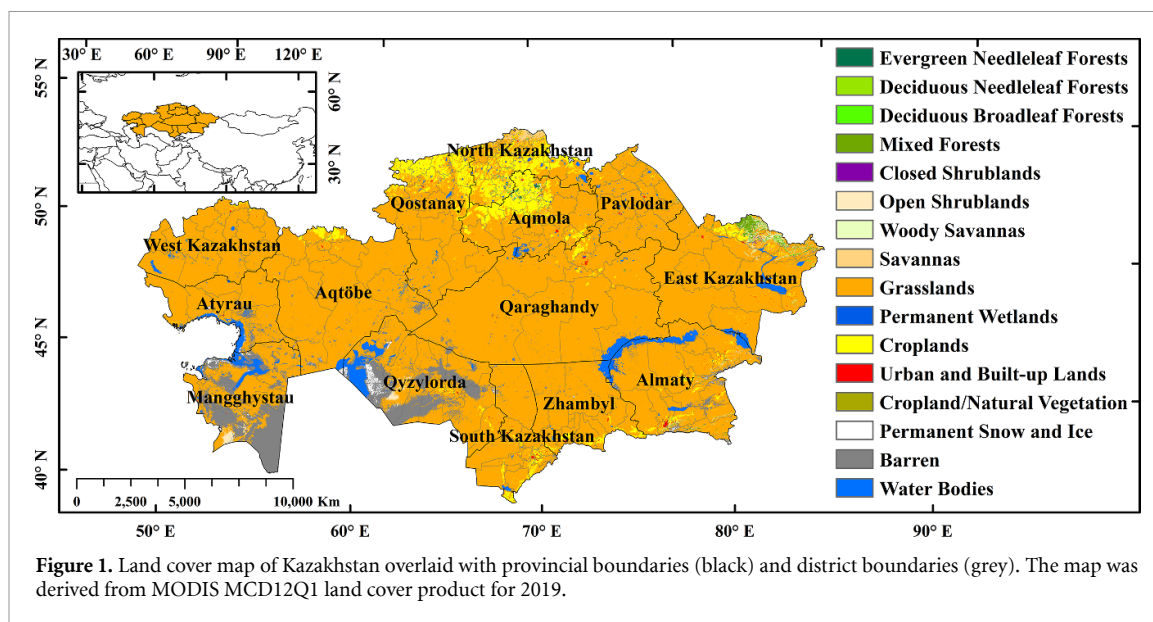
Kazakhstan is an important land-locked dryland Asian country owing to its large size and economy (Schierhorn *et al* 2020). Previous studies have found that cropland conversions, land abandonments, and livestock density trends in Kazakhstan were some of the significant factors causing land degradation (de Beurs *et al* 2015, Rolinski *et al* 2021). Kazakhstan lost a lot of cropland cover due to socio-political and structural changes in the agricultural sector during the disintegration of the Soviet Union (Frühauf *et al* 2020). For e.g. crop yields dropped from 23.4 to 10.7 million tons and heads of livestock decreased from 48.6 to 14.5 million heads between 1990 and 2000 in Kazakhstan (Kraemer *et al* 2015). Livestock management in Kazakhstan is diverse with soviet-style feedlot-based ranching systems being the predominant type. However, private ranch owners cannot afford to move livestock to prime pastures in remote areas, which could alleviate grazing pressures. This is partially explained by the lack of infrastructure and funds to rebuild abandoned watering systems as well as rural outmigration (Dara *et al* 2020). On the other hand, livestock herders in eastern Kazakhstan have been engaging in transhumance—moving livestock to different ecological zones and from lower to higher elevations—to capture the benefits of seasonally accessible forage resources (Hankerson *et al* 2019). The availability of these forage resources depends on precipitation that occurs outside of the peak growing season; thus, the variation in seasonal precipitation greatly affects vegetation production (Tomaszewska and Henebry 2020). Furthermore, increasing temperatures have triggered snow cover and glacier mass loss which is expected to accelerate further (Luo *et al* 2019). Clearly, examining the variability in seasonal rainfall and snow cover in these grassland ecosystems is increasingly crucial, as they impact seasonal and long-term water storage, vegetation phenology and pasture productivity (Qi *et al* 2017, Petersky *et al* 2019).

The vegetation-precipitation relationship (VPR) in drylands has been the primary focus of research for many decades (John *et al* 2013, 2016). Substantial changes in ecosystem structure and function of vegetation (ESF; list of abbreviations in appendix) has led researchers to evaluate the dynamics of greenness (normalized difference vegetation index—NDVI), water fluxes (evapotranspiration—ET) and ecosystem production (net primary productivity—NPP) in the context of trends in surface temperature, solar radiation, relative humidity, and vapor pressure deficit (Kong *et al* 2017, Chen *et al* 2020). These studies suggest that precipitation variability is significantly responsible for alterations in ESF variables (NDVI, ET, and NPP). In addition, studies that investigated the impacts of spring drought on ecosystem carbon dynamics in semi-arid areas also found that this phenomenon had significant socio-ecological impacts (e.g. Zhang *et al* 2012, Liu *et al* 2019). Snow cover, in addition to rainfall, is a key driver in Central Asia. Snowfall in Central Asia exceeds rainfall and is the prime contributor to the early summer soil moisture (SM) that drives seasonal biomass in pastoral lands (Apel *et al* 2018). Recent studies have explored the effects of snow cover change on vegetation over Central Asian regions (Venkatesh *et al* 2022). Most of these studies, conducted using remote sensing techniques and products, concluded that snow cover dynamics alter NPP (Wang *et al* 2018, Qiao and Wang 2019). Hence, we sought to investigate whether winter percent snow cover and spring season precipitation affect peak season greenness in Kazakhstan using a causal model.

Previous research has focused on structural (e.g. measured by vegetation optical depth—VOD) and water retention (e.g. terrestrial water storage—TWS and SM) driver impacts on vegetation changes in different ecosystems (Deng *et al* 2020, Ugbaje and Bishop 2020). Studies in dryland ecosystems have found a strong relationship between VOD and anthropogenic effects in the context of global climate change (Andela *et al* 2013, Liu *et al* 2013). The SM, TWS—vegetation relationships are also crucial as intensive water withdrawals for irrigation often alter the water cycle components, particularly in water-limited ecosystems. Previous studies have examined the individual effect of seasonal variations in moisture and water content drivers on vegetation greenness in Central Asia (Xie *et al* 2019). However, there has not been a comprehensive examination of the combined impact of moisture factors on greenness in Kazakhstan.

Scientific studies concerning the interactive effects of social-environmental system (SES) drivers on ESF changes are scarce, with only a few assessing either the effect of hydrological drivers (Xie *et al* 2016, Zheng *et al* 2019) or land cover/use change (John *et al* 2018, Dong *et al* 2020) on vegetation. Some studies have focused on coupled natural and human systems to investigate the complex ecosystem processes in semi-arid regions (Groisman *et al* 2009, Chen *et al* 2015a, 2015b). They suggest that socioeconomic changes or anthropogenic disturbances have

Figure 1. Land cover map of Kazakhstan overlaid with provincial boundaries (black) and district boundaries (grey). The map was derived from MODIS MCD12Q1 land cover product for 2019.

produced more drastic impacts than climate change in recent years (Chen *et al* 2021, Dong *et al* 2021). It is therefore necessary to examine the implications of these drivers on ESF dynamics in Kazakhstan, a country that has experienced significant land degradation and agricultural land abandonment (Prishchepov *et al* 2013, Hu *et al* 2020). A detailed analysis of the direct and indirect causal relationships between SES (climate, structural, water retention and socioeconomic) drivers and ESF response is needed and notably lacking over Central Asian areas (Tomaszewska *et al* 2020, Chen *et al* 2022).

In this study, we propose the following hypotheses to test whether there is a relationship between peak season greenness, spring precipitation and preceding winter snow cover for Kazakhstan and how this relationship is associated with land cover/use change (LCLUC): (H1) ESFs are positively and directly associated with spring precipitation and preceding winter snow cover; (H2) SM and structural water content (vegetation optical depth) have a strong influence on ESF dynamics; and (H3) Human influence has a more substantial and direct impact than climatic drivers on ESF changes.

We employed structural equation modeling (SEM) to help identify the combined interactive influences between SES drivers and the seasonal effect of these drivers on response variables (NDVI, NPP and ET). Our conceptual foundation of this integrated study of biophysical, climatic, and socioeconomic indicators driven by seasonal variation and change seeks to explain interconnectivity within coupled human and natural systems. We ask the following questions: (1) Does snow cover from the preceding winter and spring rainfall contribute jointly to peak season greenness and productivity? (2) Do socioeconomic indicators have a more substantial influence than precipitation in a water-limited ecosystem like Kazakhstan? (3) Does SM have a stronger impact than

TWS on vegetation growth in this dryland region? and (4) Is vegetation affected by changes in anthropogenic water withdrawals (TWS) and water stress (VOD) in Kazakhstan? The study area description, as well as the dataset source and resolutions are listed in figure 1, table 1 and the appendix (sections 'Study area' and 'Data sources').

2. Methods

We implemented Mann–Kendall trend (MK) and Sen's slope estimator (SS) to identify monotonic upward or downward trends in the SES variables. We calculated standardized anomalies (Z) of all input datasets to maintain consistency. These standardized anomalies were used as input in SEM. More details regarding MK, SS and standardized anomalies are represented in the appendix (sections 'Mann–Kendall trends and standardized anomalies').

We carried out SEM analysis in two different phases by analyzing the interrelationships of ESF variables with various drivers at the provincial level in Kazakhstan (Fan *et al* 2016).

Phase 1: The first phase considers the two key drivers—precipitation and percent snow cover—as latent variables (description in appendix section 'Structural equation model (SEM)').

Phase 2: The second phase considers precipitation and percent snow cover as SEM moderators. We suggest that these two potential drivers alter the relationship between ESF and other water retention, structural and socioeconomic drivers. Though many previous studies identified that precipitation and percent snow cover would affect ESF, to our knowledge, its role as SEM moderator (appendix section 'Structural equation model (SEM)') has not been explored.

In the first phase, we developed eight SEM models, considering greenness (NDVI) as the response variable. Model-1 consists of four latent constructs

Table 1. List of variables (covariates) along with source and spatial resolutions and latent groups (factors) used for structural equation modeling (SEM).

Factors	Covariates	Source	Units/spatial resolution	References
Greenness, carbon/water fluxes	Normalized difference vegetation index	MODIS (MOD13A2) https://lpdaac.usgs.gov/products/mod13a2v006/	1 km × 1 km	LPDAAC
	Evapotranspiration	MODIS (MOD16A2) https://lpdaac.usgs.gov/products/mod16a2v006/	500 m × 500 m	LPDAAC
	Net primary productivity	MODIS (MOD17A3) https://lpdaac.usgs.gov/products/mod17a3hv006/	500 m × 500 m	LPDAAC
Climate/moisture	Precipitation (Spring and Summer)	ERA—5 https://cds.climate.copernicus.eu/cdsapp#!/home	0.25 × 0.25 degree	(Hersbach *et al* 2019)
	Snow (Winter)	MODIS (MOD10A1.006) https://nsidc.org/data/MOD10A1/versions/6	500 m × 500 m	(Hall and Riggs 2016)
Water content and storage	Soil moisture	ESA-CCI www.esa-soilmoisture-cci.org/	0.25 × 0.25 degree	(Dorigo *et al* 2017)
	Vegetation optical depth	VODCA https://essd.copernicus.org/articles/12/177/2020/	0.25 × 0.25 degree	(Moesinger *et al* 2020)
	Terrestrial water storage	GRACE and GRACE—FO https://grace.jpl.nasa.gov/	1 × 1 degree	(Landerer and Swenson 2012)
Heat Stress	Air temperature	ERA—5 https://cds.climate.copernicus.eu/cdsapp#!/home	0.25 × 0.25 degree	(Hersbach *et al* 2019)
	Land surface temperature	GLDAS Noah LSM https://disc.gsfc.nasa.gov/	0.25 × 0.25 degree	(Beaudoing and Rodell 2020)
Human Influence	Crop production Population Density Gross domestic productivity Livestock density	Agency for Strategic planning and reforms of the Republic of Kazakhstan Bureau of National Statistics	Tons/hectares Population sq.km^{-1} GDP/per capita Head of Livestock/area of aimag	https://stat.gov.kz/

(LC) (supplementary figure S4(a)): (a) percent snow cover (SNOWc) under PSNOW, (b) spring precipitation (P_MAM) under PRECP, (c) livestock density (LSK$_D$), under human influence—1 or HINF1 and (d) human influence—2 (HINF2) which includes population density (POP$_D$), gross domestic product per capita (GDPca) and crop yield per hectare (CROPh). LSK$_D$ might negatively impact ESF and therefore be grouped under HINF1. Other socioeconomic variables were grouped as a separate LC (HINF2), assuming a positive impact on greenness. Furthermore, the eight SEM models were developed with multiple driving variables added to the base model (Model-1) so that the subsequent models

increased in complexity (details in appendix section 'Structural equation model (SEM)'). The driving variables were tested for influences using SEM and were removed if they were found to be non-significant or reduced model fit. The eight models with NDVI as a response are represented in table 3. Altogether, 24 SEM models were tested in the first phase of the analysis as we tested the interactions between drivers and three response (NDVI, NPP and ET) variables.

In our second phase, we developed four SEM models by considering percent snow cover and seasonal precipitation as SEM moderators. The mean and variance of spring precipitation (P_MAM and P_MAM$_{SD}$) and snow cover (SNOWc and

Table 2. Mann–Kendall Tau (τ), Sen's slope estimate and *p*-value of socioeconomic variables for 14 provinces of Kazakhstan during 2000–2016.

Region/driver	POP$_D$			CROPh			GDPca			LSK$_D$		
	Tau	Slope	*p*	Tau	Slope	*p*	Tau	Slope	*p*	Tau	Slope	*p*
Almaty	0.97	0.3	*	0.89	0.003	*	1	612.06	*	1	0.45	*
Aqmola	0.98	0.18	*	0.35	0.009	—	1	685.95	*	0.95	0.14	*
Aqtobe	0.91	0.03	*	−0.05	0	—	0.94	485.65	*	0.63	0.1	*
Atyrau	1	0.09	*	0.98	0	*	0.97	1648.5	*	0.51	0.13	*
E. Kazakhstan	−0.83	−0.02	*	0.52	0.001	*	1	353.4	*	0.58	0.31	*
Mangghystau	1	0.12	*	0.78	0	*	0.91	791.42	*	0.25	0.04	—
N. Kazakhstan	−1	−0.09	*	0.55	0.01	*	1	305.36	*	0.86	0.18	*
Pavlodar	0.02	0	—	0.35	0.002	—	0.94	496.54	*	0.97	0.28	*
Qaraghandy	0.44	0	*	0.32	0	—	1	488.92	*	0.83	0.09	*
Qostanay	−0.82	−0.02	*	0.3	0.005	—	0.98	336.54	*	0.58	0.07	*
Qyzylorda	1	0.05	*	0.79	0	*	0.86	395.09	*	0.33	0.04	—
S. Kazakhstan	1	0.46	*	0.73	0.006	*	0.98	188.08	*	0.88	1.48	*
W. Kazakhstan	0.63	0.01	*	−0.14	0	—	0.95	617.71	*	0.97	0.25	*
Zhambyl	0.91	0.06	*	0.45	0.002	*	1	193.52	*	0.95	0.51	*

p indicates *p*-value, * indicates significant ($p < 0.05$), (—) indicates non-significant ($p > 0.05$), W. Kazakhstan indicates West Kazakhstan, N. Kazakhstan indicates North Kazakhstan, E. Kazakhstan indicates East Kazakhstan, S. Kazakhstan indicates South Kazakhstan.

SNOWc$_{SD}$) were computed across years and tested as SEM moderators between SES drivers and ESF variables. In addition to the 24 models in the first phase, 12 models were tested in the second phase of the analysis to find the interactions between driving variables, SEM moderators and ESF variables. All these 36 models from two phases were developed and tested using SEM with a *lavaan v0.6-10* package in R software (Rosseel 2012). Details regarding the SEM are represented in the appendix (section 'Structural equation model (SEM)') and the structural model implemented is illustrated in the path diagram (figure 2). More details regarding the fit statistics and SEM can be found in Fan *et al* (2016).

3. Results

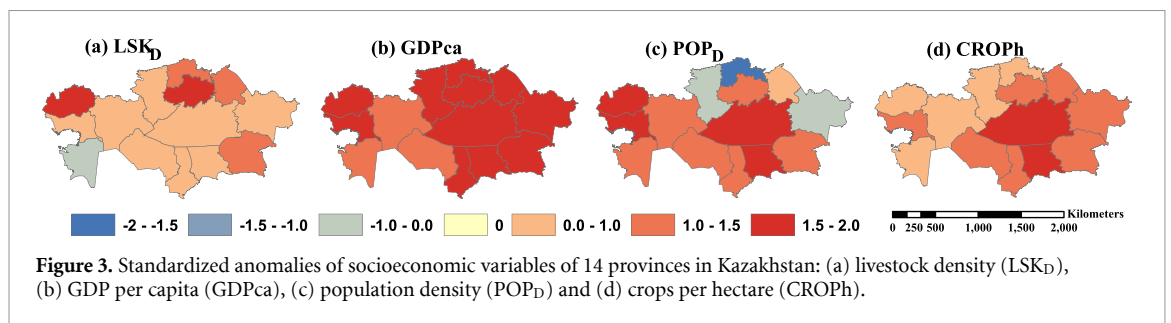### 3.1. Standardized anomalies and spatial trends of response and forcing variables

Standardized anomalies help us understand long-term spatiotemporal dynamics across various provinces in Kazakhstan. The negative anomalies of P_JJA and SM showed strong associations across various provinces in Kazakhstan (supplementary figure S1). VOD showed similar trends of NDVI, NPP and ET across Kazakhstan's eastern, western, and southern regions. Further, the negative P_MAM, VOD and NDVI anomalies over Kazakhstan's northern and southern provinces illustrated declining P_MAM and VOD effects on NDVI (supplementary figure S1). SNOWc and TWS showed similar trends with a significant increase in northern and north-eastern provinces indicating the contribution of winter snow melt water to summer ground water storage (supplementary figure S1). There was a general increase in LSK$_D$ (positive anomaly) across various provinces in

Kazakhstan (figure 3). However, significant positive anomalies of LSK$_D$ were found in West Kazakhstan and Akmola provinces. GDPca revealed significant positive anomalies across central and eastern parts of Kazakhstan (figure 3). Positive anomalies in POP$_D$ were found in most provinces in Kazakhstan except for Qostanay and East Kazakhstan provinces. CROPh exhibited positive anomalies across Kazakhstan, with significant positive anomalies in Qaraghandy and Zhambyl provinces (figures 1 and 3).

The spatial distribution of SES driver trends at the seasonal scale over Kazakhstan from 2000 to 2016 was analyzed using the MK trend test (figure 4 and supplementary figure S2). The increasing and decreasing trends were depicted in green and brown, respectively, and the significant pixels ($p < 0.05$) were represented with dots (figure 4 and supplementary figure S2). Kazakhstan has experienced a significant decrease in NDVI, NPP, ET, SM, VOD, spring and summer precipitation and a significant increase of T_{air} and LST in the western provinces of Kazakhstan. Significant greening (increasing trends of NDVI, NPP and ET) was observed in the eastern and northern provinces, along with decreasing temperatures (figure 4 and supplementary figure S2). Socioeconomic drivers, namely, POP$_D$, LSK$_D$ and GDPca significantly increased in most Kazakhstan provinces. However, crop yields showed a non-significant trend in most provinces, with only a few provinces having significantly increased CROPh trends (table 2 and supplementary figure S3). A detailed explanation on standardized anomalies, spatial MK trends and Sen's slope estimates is provided in appendix (sections 'Standardized anomalies of response and forcing variables' and 'Spatial trends of response and forcing variables').
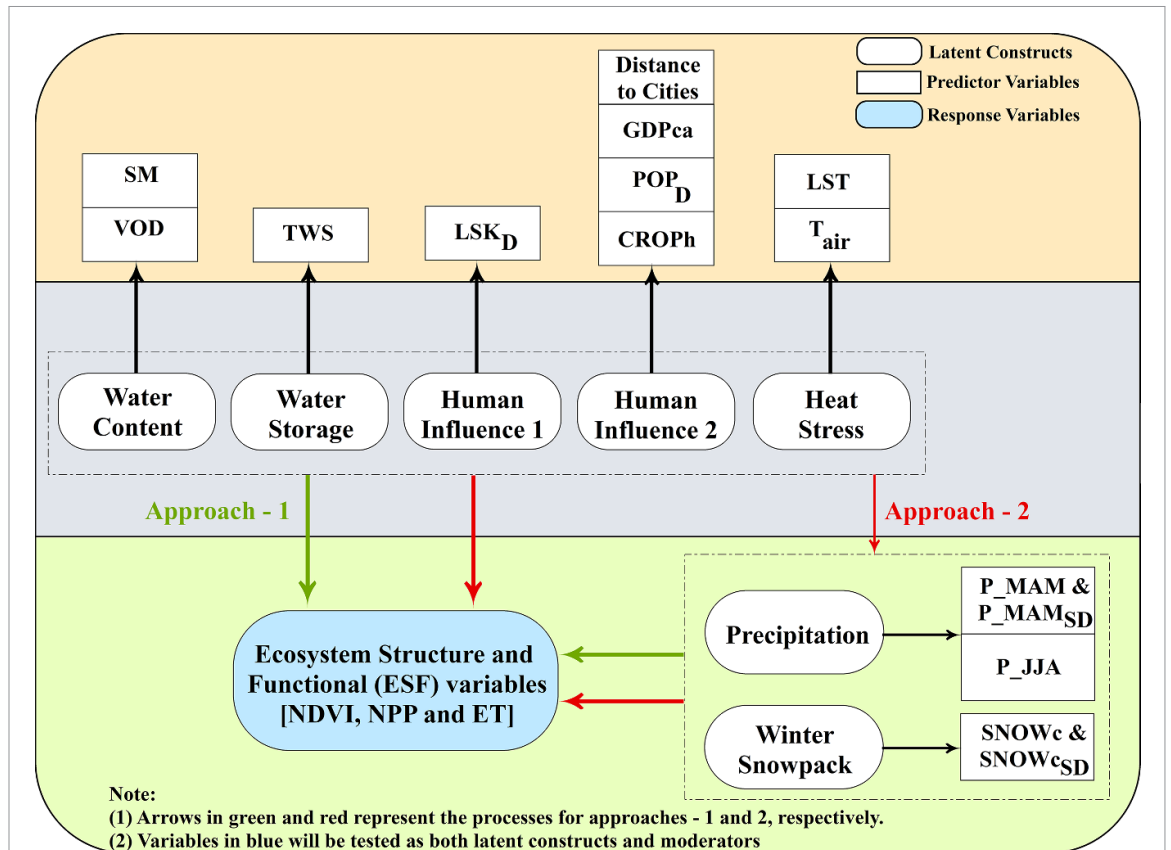
Figure 2. Structural equation model (SEM) framework investigating the possible pathways to find the interactions between predictors or drivers (climate, moisture and socioeconomic variables grouped under different latent constructs) and response variables (NDVI/NPP/ET) in this study.

(Abbreviations—normalized difference vegetation index (NDVI), net primary productivity (NPP), evapotranspiration (ET), spring precipitation (P_MAM), summer precipitation (P_JJA), percent cover snowpack (SNOWc), soil moisture (SM), vegetation optical depth (VOD), terrestrial water storage (TWS), air temperature (T_{air}), land surface temperature (LST), livestock density (LSK_D), gross domestic product per capita (GDPca), population density (POP_D), and crop production per hectare (CROPh)).

Figure 3. Standardized anomalies of socioeconomic variables of 14 provinces in Kazakhstan: (a) livestock density (LSK_D), (b) GDP per capita (GDPca), (c) population density (POP_D) and (d) crops per hectare (CROPh).

3.2. Joint interactions between ESF and driving variables

3.2.1. Phase 1: precipitation and snow cover as latent variables

The SEM model-1 indicated that P_MAM and LSK_D (HINF-1; abbreviations in appendix) had a strong positive and strong negative influence with NDVI (standardized path coefficients (SPC) of 0.68 and −0.51)(supplementary figure S4(a)). On the other hand, joint interactive influence of POP_D, CROPh and GDPca under HINF-2 showed a significant positive influence on NDVI (SPC of 0.44). Finally, winter SNOWc showed a weaker positive influence on summer NDVI in model-1 (SPC of 0.06).

Similarly, multiple models (model-2 to model-8; table 3) were tested by introducing P_JJA (model-2), VOD (model-3), SM (model-4), TWS (model-5), T_{air} (model-6), and LST (model-7) as driving variables in SEM. These details were provided in appendix section 'Precipitation and snow cover as latent variables (model 2–model 7)'. The proximity variable (D_{CITY}), added in model-8 (table 3, supplementary figure S4(h)), did not result in either a significant positive or negative influence on NDVI, though it did improve model fit (table 3, RMSEA from 0.16 to 0.11). Model-8 exhibited better model fit statistics when compared to the other models in the first phase of the analysis (table 3). Therefore, the latent variables

Figure 4. Mann–Kendall trends of ESF and driver variables for Kazakhstan during 2000–2016. Dots indicate pixels with significant *p*-value ($p < 0.05$). Abbreviations same as in figure 2.
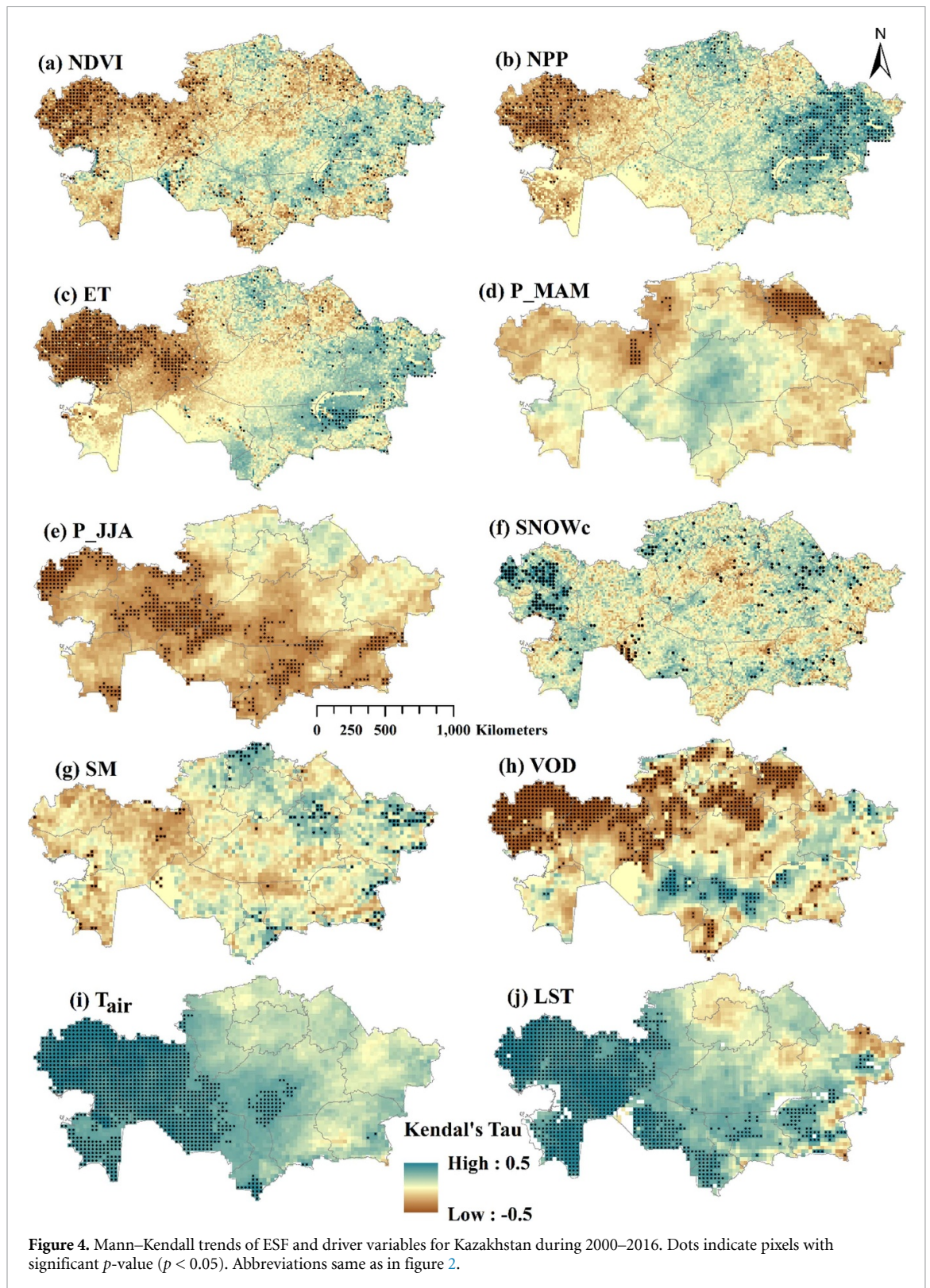
of model-8 were further employed to test the effect of SEM moderators on greenness in the second phase of the analysis.

3.2.2. Phase 2: precipitation and snow cover as SEM moderators

SEM moderator variables (P_MAM and SNOWc) were introduced to investigate the changes in interactions between latent variables and NDVI across years (models 9 through 12, table 3). Snow cover variability (SNOWc$_{SD}$, figure 5, model-12) exhibited better model fit than mean P_MAM (model-9, supplementary figure S5(a)), P_MAM variability (P_MAM$_{SD}$, model-10 from table 3 and supplementary figure S5(b)) and mean SNOWc (model-11, table 3 and supplementary figure S5(c))

Table 3. Structural equation model performance examining peak season (JJA) normalized difference vegetation index (NDVI) as response. For each SEM model, the Akaike information criterion (AIC), comparative fit index (CFI), Tucker–Lewis index (TLI), standardized root mean square residual (SRMR) and root mean square error of approximation (RMSEA) describing model performance are listed (full forms in appendix).

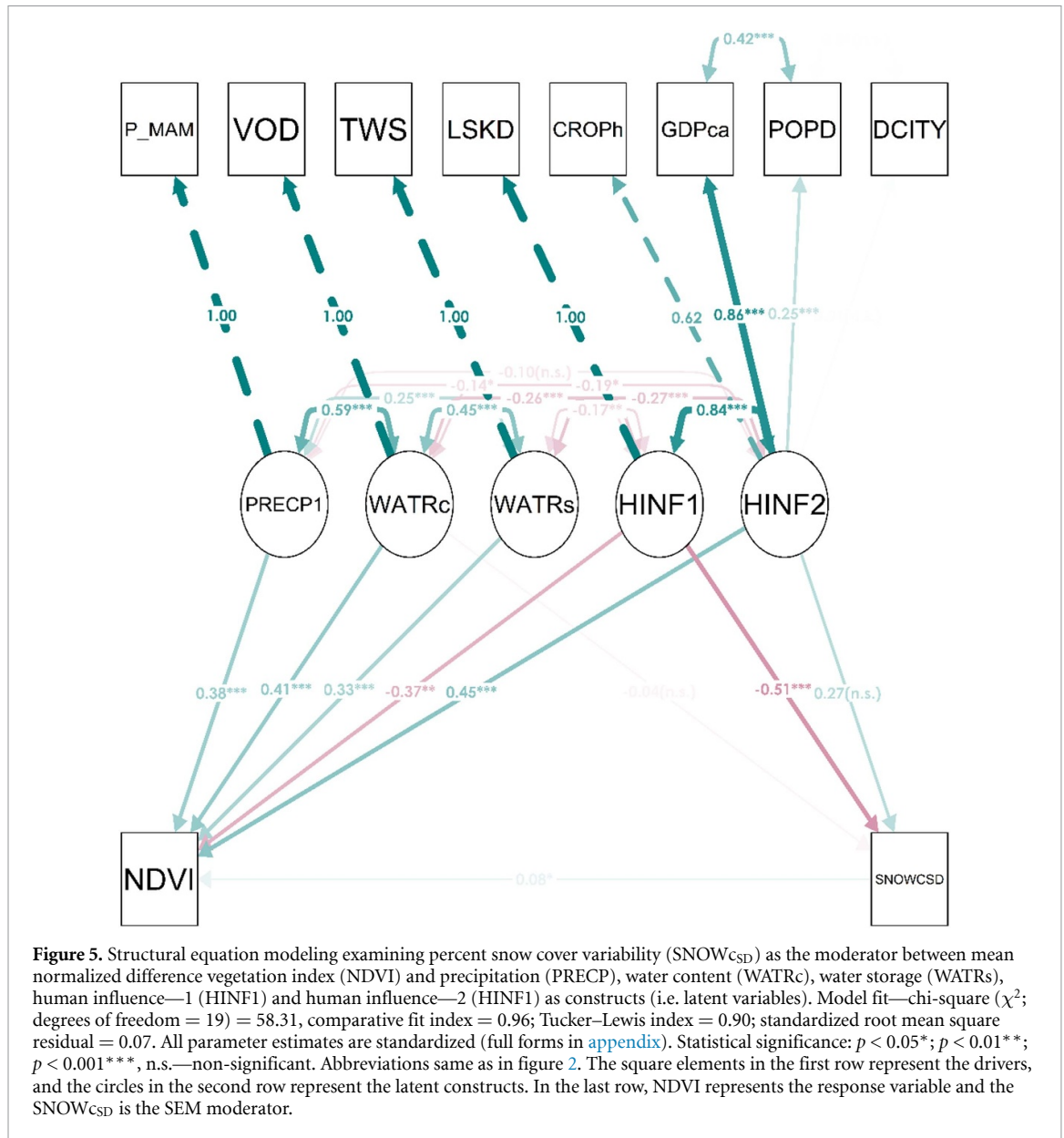| SEM model	Measurement model with NDVI	AIC	CFI	TLI	SRMR	RMSEA
1	P_MAM + SNOWc + HINF-1 + HINF-2	4143.37	0.93	0.78	0.07	0.16
2	P_MAM + P_JJA + SNOWc + HINF-1 + HINF-2	4667.36	0.93	0.78	0.07	0.15
3	P_MAM + Water Content (VOD) + SNOWc + HINF-1 + HINF-2	4083.44	0.94	0.80	0.08	0.16
4	P_MAM+ Water Content (VOD + SM) + SNOWc + HINF-1 + HINF-2	4589.10	0.91	0.79	0.09	0.16
5	P_MAM + Water Content (VOD) + Water Storage (TWS) + SNOWc + HINF-1 + HINF-2	4557.94	0.94	0.79	0.08	0.15
6	P_MAM + Water Content (VOD) + Water Storage (TWS) + SNOWc + HINF-1 + HINF-2 + Heat Stress (T_{air})	5113.44	0.93	0.74	0.09	0.16
7	P_MAM + Water Content (VOD) + Water Storage (TWS) + SNOWc + HINF-1 + HINF-2 + Heat Stress (LST and T_{air})	5326.05	0.91	0.76	0.10	0.17
8	P_MAM + Water Content (VOD) + Water Storage (TWS) + SNOWc + HINF-1 + HINF-2 (D_{CITY} added)	4421.86	0.94	0.87	0.08	0.11
	WITH SEM MODERATOR					
9	P_MAM (moderator) + Water Content (VOD) + Water Storage (TWS) + SNOWc + HINF-1 + HINF-2 (D_{CITY} added)	4406.35	0.96	0.91	0.07	0.09
10	P_MAM$_{SD}$ (moderator) + Water Content (VOD) + Water Storage (TWS) + SNOWc + HINF-1 + HINF-2 (D_{CITY} added)	4505.89	0.95	0.90	0.07	0.09
11	SNOWc (moderator) + Spring Precipitation + Water Content (VOD) + Water Storage (TWS) + HINF-1 + HINF-2 (D_{CITY} added)	4413.90	0.95	0.88	0.07	0.1
12	SNOWc$_{SD}$ (moderator) + Spring Precipitation + Water Content (VOD) + Water Storage (TWS) + HINF-1 + HINF-2 (D_{CITY} added)[a]	4387.51	0.96	0.90	0.07	0.09

[a] Model with the lowest AIC and best performance. T_{air}, air temperature; LST, land surface temperature, D_{CITY}, distance to city.

when tested as SEM moderators. We found the influence of socioeconomic variables on NDVI while moderated by an increasingly variable climate (precipitation or snow cover as SEM moderators). In model-12, LSK$_D$ showed a strong negative influence (SPC of −0.51) on NDVI through the moderating effect of SNOWc$_{SD}$. LSK$_D$ has a direct negative impact of −0.37 on NDVI, whereas it was increased to −0.51 under the influence of snow cover (moderator). Similarly, HINF-2 has a direct positive influence of 0.45 on NDVI and decreases to 0.27 when snow cover was introduced as a moderator. In contrast, no significant impacts were found for WATRc and WATRs LC with NDVI through SNOWc$_{SD}$. It was further observed that socioeconomic variables (HINF-1 and HINF-2) showed a stronger influence (SPC of −0.37 and 0.45) on NDVI when compared to WATRc, WATRs and PRECP LC (SPCs of 0.41, 0.33 and 0.38) through SNOWc$_{SD}$ as SEM moderator (figure 5). The statistical fit of model-12 with SNOWc$_{SD}$ as SEM moderator exhibited the overall best fit of all the 12 models tested with NDVI as a response (table 3).

The two-phase analysis described in section 2 was repeated to test the interactions between predictor variables, NPP and ET. We found that model-12 with SNOWc$_{SD}$ (figures 6 and 7) as SEM moderator exhibited better performance in terms of lower AIC (4485.56 & 4458.43), SRMR (0.07 & 0.07), and RMSEA (0.1 & 0.09) values for NPP and ET, respectively (supplementary tables 1 and 2). We also found that socioeconomic drivers had a more substantial and direct influence on productivity (SPC of −0.51 and 0.81 for HINF-1 and HINF-2) when compared to climatic and water retention parameters.

We observed key differences in driving factor impacts on response variables (NDVI, NPP and ET) (figures 5–7). We found a strong direct positive influence of HINF-2 on NDVI, followed by VOD and P_MAM. We also found a strong indirect negative influence of HINF-1 on NDVI through SNOWc$_{SD}$ (figure 5). For NPP, we found that HINF-2 had a strong direct positive impact, followed by HINF-1 and VOD. In contrast, the influence of P_MAM on NPP was weaker (figure 6). Similar to NDVI, HINF-1 exhibited a strong indirect negative influence on NPP through SNOWc$_{SD}$. While HINF-2 had a strong direct positive impact on ET, followed by all three moisture drivers (VOD, TWS and P_MAM), we

Figure 5. Structural equation modeling examining percent snow cover variability (SNOW$_{SD}$) as the moderator between mean normalized difference vegetation index (NDVI) and precipitation (PRECP), water content (WATRc), water storage (WATRs), human influence—1 (HINF1) and human influence—2 (HINF1) as constructs (i.e. latent variables). Model fit—chi-square (χ^2; degrees of freedom = 19) = 58.31, comparative fit index = 0.96; Tucker–Lewis index = 0.90; standardized root mean square residual = 0.07. All parameter estimates are standardized (full forms in appendix). Statistical significance: $p < 0.05*$; $p < 0.01**$; $p < 0.001***$, n.s.—non-significant. Abbreviations same as in figure 2. The square elements in the first row represent the drivers, and the circles in the second row represent the latent constructs. In the last row, NDVI represents the response variable and the SNOW$_{SD}$ is the SEM moderator.

found that the influence of LSK$_D$ on ET was weaker (figure 7). In summary, VOD and HINF-2 showed a strong direct positive influence and HINF-1 exhibited strong indirect negative influence on ESF variables.

3.3. Joint interactions between SEM latent constructs

The lateral covariances between predictor variables were best explained by model-12 (figure 5). P_MAM indicated a strong positive covariance with WATRc (SPC of 0.59), WATRs (SPC of 0.25) and negative covariance with HINF1 (SPC of −0.14) and HINF-2 (SPC of −0.1) variables. WATRc exhibited a strong positive covariance with WATRs (0.45) and a negative relationship with HINF-1 (SPC of −0.25) and HINF-2 (SPC of −0.19). On the other hand, WATRs had a significant negative covariance with HINF-1 (SPC of −0.17) and HINF-2 (SPC of −0.27) LC.

Finally, the joint interactions between socioeconomic variables, HINF-1 and HINF-2, exhibited strong positive covariance with an SPC of 0.84 (figure 5).

3.4. Hypotheses testing

Model-12 (table 3, supplementary tables 1 and 2), which exhibited the best model fit, was used to test our framed hypotheses. *Hypothesis 1:* P_MAM and SNOW$_{SD}$ showed a positive impact on NDVI (SPC of 0.38 and 0.08), NPP (SPC of 0.21 and 0) and ET (SPC of 0.36 and 0.09). These results suggest that the proposed hypothesis (H1) can be accepted as both P_MAM and SNOWc had a significant positive impact ($p < 0.05$) on NDVI. *Hypothesis 2:* Soil moisture was removed from the final model as it resulted in poor model fit statistics. However, both SM and VOD showed a strong influence on NDVI (SPC of 0.46—supplementary

Figure 6. Structural equation modeling examining percent snow cover variability ($SNOW_{cSD}$) as a moderator between the mean net primary productivity (NPP) and precipitation (PRECP), water content (WATRc), water storage (WATRs), human influence—1 (HINF1) and human influence—2 (HINF2) as constructs (i.e. latent variables). Model fit—chi-square (χ^2; degrees of freedom = 19) = 61.31, comparative fit index = 0.95; Tucker–Lewis index = 0.89; standardized root mean square residual = 0.07. All parameter estimates are standardized (full forms in appendix). Statistical significance: $p < 0.05^*$; $p < 0.01^{**}$; $p < 0.001^{***}$, n.s.—non-significant. Abbreviations same as in figure 2.

figure S6(a) and 0.58—supplementary figure S6(b)), NPP (SPC of 0.55—supplementary figure S6(c) and 0.63—supplementary figure S6(d)) and ET (SPC of 0.47—supplementary figure S6(e) and 0.56—supplementary figure S6(f)). These results suggest that the H2 can be accepted as SM and VOD had a stronger impact on ESF variables. *Hypothesis 3:* We can accept our third hypothesis as socioeconomic variables under HINF-2 showed a more substantial impact than climatic drivers when interacting with ESF variables (figures 5–7). In addition, HINF-1 showed a stronger impact than climatic drivers when interacting with NPP and a similar impact to climatic drivers when interacting with NDVI (figures 5–7).

Our research addressed the four research questions that were framed in the introduction. We found that (1) spring rainfall had a stronger impact on ESF variables than winter snow cover (figures 5–7). However, we also found that the variance in winter snow cover has a higher influence on NDVI than spring precipitation (Model 12 was better than Model 9 and 10), (2) socioeconomic variables (HINF-1 and HINF-2) had a more substantial impact on ESF variables than precipitation in Kazakhstan (figures 5–7), (3) summer ground water storage showed a stronger influence than SM on NDVI (SPC of 0.31 and 0.27—supplementary figure S7(a)) and ET (SPC of 0.38 and 0.25—supplementary figure S7(c)), and (4) both TWS and VOD have significantly contributed to the changes in ESF variables (figures 5–7). However, VOD showed a stronger impact than TWS on NDVI (SPC of 0.41 and 0.33; figure 5), NPP (SPC of 0.46 and 0.38; figure 6) and a weaker impact on ET (SPC of 0.37 and 0.39; figure 7) in Kazakhstan.

Figure 7. Structural equation modeling examining percent snow cover variability (SNOWc$_{SD}$) as a moderator between the evapotranspiration (ET) and precipitation (PRECP), water content (WATRc), water storage (WATRs), human influence—1 (HINF1) and human influence—2 (HINF2) as constructs (i.e. latent variables). Model fit—chi-square (χ^2; degrees of freedom = 19) = 55.26, comparative fit index = 0.96; Tucker–Lewis index = 0.90; standardized root mean square residual = 0.07. All parameter estimates are standardized (full forms in appendix). Statistical significance: $p < 0.05^*$; $p < 0.01^{**}$; $p < 0.001^{***}$, n.s.—non-significant. Abbreviations same as in figure 2.

4. Discussion

Our research employed SES modeling to better understand vegetation dynamics in semi-arid regions. First, we used latent constructs to develop indicators that represent meaningful and complementary characteristics of SES drivers. Second, we tested the role of SEM moderators in explaining joint interactions of drivers on response variables. While the estimated latent construct values are site-specific, our methods suggest an approach to reduce predictor variables to represent vegetation ESF. Our findings could help guide researchers in prioritizing data collection if only a limited number of variables can be obtained. Such dimensionality reduction can be implemented in other water-limited ecosystems to improve sampling and interpretation capabilities.

4.1. Joint interaction of seasonal rainfall and winter percent snow cover on ESF

Very few studies have focused on coupled natural and human systems to explore the complex ecosystem processes that include the climatic and socioeconomic drivers in Central Asia. Some efforts have been made at smaller scales in Mongolia (Fernández-Giménez *et al* 2018), Inner Mongolia (Wang *et al* 2017, Yan *et al* 2020b), and Uzbekistan (Yang *et al* 2016). Most of these studies used either regression models or trend analysis to examine the contribution of climatic and socioeconomic drivers to vegetation dynamics (Zhang *et al* 2020, Guo *et al* 2021). In contrast, we identified the joint interactive influences between SES drivers and the seasonal effect of these drivers on ESF using SEM in Kazakhstan. Our results showed that rainfall has a strong and significant positive influence on ESF across provinces

in Kazakhstan. We also found that spring rainfall (P_MAM) contributed to increased greenness when compared to summer rainfall (P_JJA). The MK results also showed that NDVI and ET had similar trends of P_MAM. This was due to the significant time it takes for rainfall to convert into sub-surface moisture and contribute to vegetation growth (Zhang *et al* 2012, Zhou *et al* 2015). These inter-seasonal relationships are in agreement with previous studies that have attempted to analyze the influence of seasonal rainfall on vegetation in semi-arid ecosystems (Wen *et al* 2019, Shi *et al* 2021, Venkatesh *et al* 2022).

Our findings also highlight that winter SNOWc has a significant but weak positive influence on peak season ESF in Kazakhstan. This could be due to ephemeral snowpacks that persist for less than 60 d (Petersky *et al* 2019). These ephemeral snowpacks have minimal predictable timing, and the snowmelt before the end of winter lowers the soil water availability for the peak growing summer season vegetation. Solomon *et al* (2009) suggested that with increasing spring and winter temperatures, precipitation would occur as rain rather than snow, particularly at the start and end of the winter, thereby enhancing the impact of rainfall on vegetation rather than snow. A similar phenomenon was observed in parts of Central Asia, as described by Chen *et al* (2016) and Tomaszewska *et al* (2020), indicating that the transition of snow to rain results in reduced snow and glacier ice accumulation during the winter. The MK spatial trends support these results as we found a reduction of SNOWc in most provinces of Kazakhstan.

We found that SNOWc has significant negative interaction with LSK_D. This negative influence can be attributed to livestock deaths due to increased competition for natural forage and decreased quality and quantity of winter food availability during harsh winters in Kazakhstan (Hauck *et al* 2016, Mirzabaev *et al* 2016). The increase in frequency and severity of anomalous snow cover events due to significant warming and drying trends over Central Asia (e.g. Kazakhstan, Mongolia and Tibet) have caused high LSK_D mortality rates (Wang *et al* 2013, Nandintsetseg *et al* 2018).

4.2. Joint interaction of SM, VOD and TWS on ESF
Our SEM modeling indicated that SM has a strong and significant positive influence on ESF and strong positive covariance with P_MAM, VOD and TWS drivers. The MK trends also showed that SM had a similar spatial trend as VOD, NDVI, NPP and ET variables. The positive interaction between SM and vegetation suggests that the plant canopy had the function of water retention and storage. A similar positive feedback mechanism between SM trend and vegetation greening was earlier suggested by Li *et al*

(2018) and Deng *et al* (2020). This positive feedback mechanism prevents extended soil drying, improves productivity and further prevents desertification and droughts.

We found that VOD has a significant positive relationship with ESF and strong positive covariance with SM, TWS and precipitation. These findings from SEM are similar to the results of MK spatial trends. This suggests that the alterations in moisture and storage variables affect vegetation water content, thereby affecting plant growth and productivity (Konkathi and Karthikeyan 2022). These results agree with the studies that employed VOD to understand vegetation dynamics in different ecosystems (Andela *et al* 2013, Tian *et al* 2018). The reduction of grassland canopy cover can explain the strong negative covariance between VOD and LSK_D through overgrazing which strongly reduces plant water content (Liu *et al* 2013, Zhou *et al* 2018). Future studies could perhaps focus on measuring the VOD variability at the early plant growth stage, which might help estimate the grassland canopy productivity at the end of the peak growing summer season.

Our findings show that TWS has a significant positive influence on ESF. These findings are in agreement with previous studies that found a strong positive relationship between TWS and NDVI compared to SM and precipitation during summer (A *et al* 2015, Ugbaje and Bishop 2020). This strong positive relationship might be due to summer precipitation failing to establish a stronger connection with TWS that contributes to vegetation growth. In addition, vegetation growth could either diminish the available SM or convert to ET due to heat stress. This forces vegetation to depend on root zone water storage for survival, thereby exhibiting a strong relationship with TWS during the peak growing summer season. Hence, we suggest that examining TWS dynamics were equally important compared to the changes in precipitation and SM. We also found strong negative covariance between POP_D, GDPca and TWS. This suggests an increase in water withdrawal and intensive irrigation agriculture, driven by increased population growth (Sun *et al* 2020). Future research could focus on measuring groundwater withdrawal rates in Kazakhstan as this is a major knowledge gap.

4.3. Joint interaction of socioeconomic drivers on ESF
We found a general increase in LSK_D anomalies across provinces in Kazakhstan. The MK trends also showed a significant increase in LSK_D in most provinces of Kazakhstan. This LSK_D increase suggests higher grazing intensities that might cause a substantial decline in grassland plant diversity, NPP and resilience

(Fetzel *et al* 2017, Liang *et al* 2018). Our SEM results also indicated that LSK_D had a strong negative influence on ESF variables compared to other driving variables. Our results agree with the previous findings that grazing was a significant factor contributing to the decline in primary production compared to precipitation (Dangal *et al* 2016, Liang *et al* 2018). However, more research is needed to determine whether certain grazing patterns affect vegetation growth, particularly those used during the peak growing season.

We also found a strong positive covariance between GDPca, POP_D and LSK_D. The MK trends showed that these three socioeconomic drivers are significantly increasing in most provinces of Kazakhstan. This can be attributed to the rapid increase in livestock density (figure 3(a)) to meet the demand for meat by a growing population (Flammini *et al* 2013, Sans and Combris 2015). Recent studies found that many countries have transitioned from cereal-dominated diets to a rise in meat consumption following an increase in economic growth (Qi *et al* 2017). Such an increase in livestock density and subsequent intensive grazing has led to degradation of grassland ecosystems in Kazakhstan.

Our findings highlight the positive anomalies in CROPh and GDPca that could be explained by increased crop yields in Kazakhstan. The country experienced a drastic increase in croplands from 8% to 54% during 1953–1990, especially following the Soviet Union's virgin lands campaign in the 1960s (Swinnen *et al* 2017). In the 1990s, Kazakhstan experienced a drastic decline in cropland use after transitioning from state-ownership to a market economy. This resulted in a loss of assured markets, disintegration of value chain supplies, and deterioration of pricing linkages between inputs and outputs (Frühauf *et al* 2020). In addition, a reduction in livestock density and the demand for fodder drove a reduction in crop production, thus contributing to cropland abandonment during the post-Soviet period (Kraemer *et al* 2015). Increasing government support and investment in agricultural management since 2000 has led to 81% of cropland recultivation in the northern steppe region (Meyfroidt *et al* 2016). Furthermore, in southern Kazakhstan, cropland recultivation around major cities and a high percentage of irrigation agriculture near the Syr Darya river regions contributed to a sharp increase in cropland area (Klein *et al* 2012, Xi and Sokolik 2016). These findings can be further validated from the MK trends that showed a significant increase of CROPh in northern (Qostanay and Aqmola) and South Kazakhstan provinces. Though CROPh and GDPca are

rising, there are serious concerns regarding long-term sustainability in Kazakhstan, as it has limited water and energy resources for food production (Wright *et al* 2012, Chen *et al* 2015a). Grassland conversion to cropland affects water resources and causes environmental degradation due to reduced soil carbon, enhanced soil salinity and reduced groundwater levels (Lal 2011, Kulmatov 2014).

5. Conclusion

This study examined the spatiotemporal changes in ESF variables (NDVI, NPP and ET) during 2000–2016 using standardized anomalies, Mann–Kendall trends, Theil-Sen's slope estimates and structural equation modeling (SEM). We quantified direct and indirect interactions, covariances and joint influences of climatic, anthropogenic, heat stress, water storage and moisture drivers on ESF variables at the provincial scale in Kazakhstan. We found that Kazakhstan experienced a significant decrease in NDVI, NPP, ET, SM, VOD, spring and summer precipitation and a significant increase of T_{air} and LST in the western provinces of Kazakhstan. We also found a significant greening (increasing trends of NDVI, NPP and ET) in the eastern and northern provinces, along with decreasing temperatures. The socioeconomic trends showed that POP_D, LSK_D and GDPca significantly increased in most Kazakhstan provinces. However, crop yields showed a non-significant trend in most provinces, with only a few provinces having significantly increased CROPh trends. Our SEM results suggest that water content (vegetation and soil) and joint interaction of human influence factors drive vegetation changes in Kazakhstan.

(a) We hypothesized and tested the effects of spring rainfall and winter snow cover on peak season ESF. We found that spring rainfall has a dominating impact over summer rainfall on ESF changes. Snow cover did not show a strong direct positive influence on ESF variables; instead, it played a moderating role, altering the influence of socioeconomic drivers on ESF variables. (b) VOD and SM, the critical drivers for vegetation growth, exhibited a strong positive influence on ESF and strong positive covariance with P_MAM and TWS variables. We identified positive feedback between vegetation and SM, indicating that the plant canopy had the function of water retention and storage. Furthermore, we found a strong positive impact of TWS on vegetation changes in Kazakhstan, a dryland ecosystem with diminishing surface water resources. (c) We also found an increase in livestock density and its enhanced negative impact on land degradation and productivity as measured by ESF dynamics. We observed a strong positive relationship

between livestock density, population density and economic growth. This is attributable to the increased demand for livestock numbers and a growing population that has shifted its dietary habits from cereals to meat in Kazakhstan. Furthermore, positive anomalies in CROPh were explained by cropland recultivation in northern and southern Kazakhstan regions. The increase in livestock density, grassland conversions, a transition from snow to rain and strong dependence of vegetation on subsurface moisture affect water availability and causes grassland degradation in Kazakhstan. Thus, there is a need to develop alternative approaches to limit overgrazing and grassland conversion and maximize forage production in Kazakhstan.

Data availability statement

The data that support the findings of this study are available upon reasonable request from the authors.

Ethical approval

Our study does not involve human subjects and/or animals. The manuscript in part or in full has not been submitted or published anywhere.

Conflict of interest

The authors declare that they have no known competing financial interests or personal relationships that could have appeared to influence the work reported in this paper.

Appendix

Abbreviations

Variable	Full form	Category
P_MAM	Mean precipitation_MAM	Predictor variable
P_MAM$_{SD}$	Standard deviation of precipitation_MAM	Predictor variable
P_JJA	Precipitation_JJA	Predictor variable
SNOWc	Mean percent snow cover_DJF	Predictor variable
SNOWc$_{SD}$	Standard deviation of percent snow cover_DJF	Predictor variable
SM	Soil moisture	Predictor variable
VOD	Vegetation optical depth	Predictor variable
TWS	Terrestrial water storage	Predictor variable
LSK$_D$	Livestock density	Predictor variable
CROPh	Crops per hectare	Predictor variable
GDPca	Gross domestic productivity per capita	Predictor variable
POP$_D$	Population density	Predictor variable
D_{CITY}	Distance to cities	Predictor variable
NDVI	Normalized difference vegetation index	Response variable
NPP	Net primary productivity	Response variable
ET	Evapotranspiration	Response variable
PRECP	Precipitation	Latent construct
PSNOW	Winter snowcap	Latent construct
WATRc	Water content	Latent construct
WATRs	Water storage	Latent construct
HINF1	Human influence 1	Latent construct
HINF2	Human influence 2	Latent construct
SEM	Structural equation model	Model
SES	Social-environmental systems	—
ESF	Ecosystem structure and function	—
LCLUC	Land cover/use change	—
LC	Latent constructs	—
CFI	Comparative fit index	Statistical index
TLI	Tucker–Lewis index	Statistical index
SRMR	Standardized root mean square residual	Statistical index
RMSEA	Root mean square error of approximation	Statistical index
AIC	Akaike information criterion	Statistical index
SPC	Standardized path coefficients	Statistical value

Study area

Kazakhstan is the largest landlocked country (2.72 million km^2) in dryland Asia (40 −55° N, 50 −85° E). The country comprises 14 regions (i.e. provinces) with grasslands as the dominant land cover type, occupying over 1.45 million km^2 (figure 1). Kazakhstan has a typical continental arid climate with extreme winters and dry, hot summers (Yuan *et al* 2022). The annual rainfall ranges from 100 mm in arid grasslands to 200 mm in semi-arid grasslands, reaching 900 mm in montane grasslands in alpine regions (Yan *et al* 2020a). The average temperature over the country fluctuates widely, ranging from −20 °C in January in north and central regions, to 18 °C in the North and 29 °C in the South by July. It was estimated that ∼60% of Kazakhstan (i.e. ∼180 million hectares) is currently experiencing desertification (de Beurs and Henebry 2004). Prior to Soviet Union's disintegration in 1991, a few large state-owned organizations dominated agricultural production. After 1991, in spite of large cooperatives by private landowners, there were serious constraints on agricultural productivity in Kazakhstan. These were mainly due to a cessation of trading agreements; decline in regional demand for cereals and other food grains; improper planning for trade; transportation and storage; minimal government support for innovation and development in agricultural research; and higher costs for pesticides (Meng *et al* 2000, Shmelev *et al* 2021). However, by 1998 almost 98% of the croplands were managed by private landowners (Suleimenov and Oram 2000, Schierhorn *et al* 2020). These changes have led to reductions in areas under cultivation, livestock units and production of food grains (Baydildina *et al* 2000). Kazakhstan also experiences frequent droughts resulting in lowered productivity and increased interannual variability of agricultural yields (Kim *et al* 2021).

Data sources

Ecosystem, climatic and socioeconomic data records: NDVI, NPP and ET datasets were obtained from the moderate resolution imaging spectroradiometer (MODIS) dataset (table 1). Precipitation and air temperature were obtained from ECMWF reanalysis (ERA—5) datasets. Cumulative spring and summer precipitation (P_MAM and P_JJA) and mean summer air temperature (T_{air}) were computed for each year over the study period (2000–2016). Normalized difference snow index (NDSI) data were used to derive a maximum percent snow cover (SNOWc) composite over winter for each province (Hall and Riggs 2016). A merged (active and passive sensor) SM dataset from the European space agency—climate change initiative (ESA CCI) project was used in the study (table 1). The vegetation optical depth (VOD) dataset developed from X-band Radar was used to examine the structural behavior of vegetation (Moesinger *et al* 2020). We obtained TWS data

from GRACE and GRACE-FO datasets produced by NASA JPL (table 1). We also used the NASA global land data assimilation system (GLDAS) derived land surface temperature (LST) (table 1). To maintain consistency, z-scores were calculated for each dataset and processed to obtain each province's spatial mean. Socioeconomic variables, including livestock density (LSK_D), population density (POP_D), gross domestic product per capita (GDPca) and crop yield (CROPh), were obtained for each province from the Kazakhstan Bureau of National Statistics and normalized by the areal extent of the province.

Our first hypothesis was to test whether the preceding winter snow cover and spring season precipitation impacts peak season (summer) greenness. Hence, only spring (March–April–May; MAM) and summer (June, July and August; JJA) precipitation and winter snow cover (December–January–February; DJF) were considered, as Kazakhstan is a semi-arid country with moisture being a major limiting factor (supplementary figure S8).

Furthermore, Kazakhstan like most countries, has annual records, while monthly or seasonal datasets are rare. Thus, we used annual socioeconomic data that was available. Grasses/crops in semi-arid regions use surface water available in the initial phase (April–May during sprouting) from precipitation/snow and later depend on soil moisture (SM during June–July–August from supplementary figure S8) and groundwater storage during the peak growing season. Hence, we have used summer SM and terrestrial water storage (TWS) datasets in the analysis.

Mann–Kendall trends and standardized anomalies

Mann–Kendall trend (MK) and Sen's slope estimator (SS) are non-parametric statistical tests used to identify monotonic upward or downward trends in the SES variables. The MK and SS are considered robust as they (a) avoid presumptions of data distribution and data skews, (b) correct for serial autocorrelation, (c) are less sensitive to outliers and (d) can handle abrupt changes due to non-uniform time series. The MK Tau (τ) ranges from −1 to 1, with positive and negative values indicating an increasing and decreasing trend. The Sen's slope magnitude (change per unit time), either positive or negative, signifies the trend's strength. The significance of trends is determined based on the *p*-value. The null hypothesis indicating no significant trend will be rejected if the *p*-value is less than 0.05. The MK trend and Sen's slope was calculated using *Kendall, trend* and *SpatialEco* packages in R software, version 4.0.3. More details regarding the equations and usage can be found in Mann (1945), Sen (1968) and John *et al* (2016).

Anomalies are the difference between a variable's current value and the long-term mean. Standardized anomalies are obtained when these anomalies are divided by the long-term standard deviation of that variable (John *et al* 2013). We calculated standardized

anomalies (Z) of all input datasets to maintain consistency as:

$$z = \frac{x - \bar{x}}{\sigma} \qquad (1)$$

where z is the standardized anomaly of a response/-predictor variable (e.g. NDVI, SM, etc) for a specific year (2020) relative to the long-term mean ($\bar{x}$) and standard deviation (σ) from 2000 to 2016. These standardized anomalies were used as input in SEM.

Structural equation model (SEM)

The multivariate causal relationships in our SEMs were modeled by employing two or more structural equations (Fan *et al* 2016). The hypothetical dependencies between variables based on path analysis were tested using the structural model, whereas the latent variables were measured using the measurement model in SEM. Latent variables in SEM are unquantified variables whose impact can be estimated using one or more predictor variables. Latent variables are important for capturing complex system properties that are difficult to estimate physically. These latent and measured variables in SEM are framed based on theoretical knowledge and developed to test competing hypotheses regarding processes accountable for dynamics in the data (Chen *et al* 2015a). A significant advantage of SEM is that it explains the covariances among different variables instead of correlations and can handle non-linearities, hierarchical paths, categorical variables and complicating factors (Grace and Keeley 2006, Grace *et al* 2012). Furthermore, we have tested the role of SEM moderator in this study. An SEM moderator is a quantitative variable that impacts the strength of the association between a predictor and response variable (Giannico *et al* 2021).

We developed eight SEM models in the first phase of the analysis. Model-1 structure was described in section 2 and represented in supplementary figure S4(a). Model—2 introduced P_JJA under PRECP2 LC to test its impact on summer greenness (supplementary figure S4(b)). Model—3 introduced VOD as a separate LC (termed water content or WATRc) to test its association with greenness (supplementary figure S4(c)). Model—4 presents SM parallel to VOD in WATRc LC as VOD and SM are proxies of plant and soil water content, respectively (supplementary figure S4(d)). Model—5 includes a new LC (WATRs) with TWS, a proxy of water storage (supplementary figure S4(e)). Model—6 tests the influence of T_{air} (heat stress—HEATs LC), that might exert a negative impact on greenness (supplementary figure S4(f)). Model—7 introduces LST parallel to T_{air} in HEATs LC to test the combined effect of temperature on greenness (supplementary figure S4(g)). Model—8 introduces a proximity variable, i.e. distance to cities (D_{CITY}) in the HINF-2 LC (supplementary figure S4(h)). We suggest that D_{CITY} and greenness might

have a positive association, as increasing proximity to cities decreases ecological disturbance. In total, 24 models were tested in the first phase of the analysis as we are testing the associations between driving variables and three response variables (NDVI, NPP and ET). The SEM was tested for 17 years across 14 provinces with a maximum of 11 driving variables in a model. Therefore, we maintained a ratio of 238 (17 × 14):11, i.e. ~21:1 for a model with highest number of variables (table 3, supplementary tables 1 and 2). SEM goodness of fit was assessed with a chi-squared value $\left(\chi^2\right)$, comparative fit index (CFI), Tucker–Lewis index (TLI), standardized root mean square residual (SRMR), root mean square error of approximation (RMSEA) and akaike information criterion (AIC). A good model fit is defined when the CFI and TLI are >0.9, SRMR is <0.08, RMSEA is <0.06 and lower AIC among different models.

Standardized anomalies of response and forcing variables

NDVI showed significant positive anomalies across eastern and western Kazakhstan regions but negative anomalies in the southern (South Kazakhstan and Zhambyl) and over a few northern (Qostanay and Pavlodar) provinces (figure 1 and supplementary figure S1). NPP and ET showed similar trends with significant negative anomalies in the western (Atyrau and Mangghystau) and south-western (Qyzylorda) regions and positive anomalies across central and eastern parts of Kazakhstan (figure 1 and supplementary figure S1). P_MAM showed a significant increase in western and south-eastern provinces of Kazakhstan, whereas there was a significant decrease in northern regions (North Kazakhstan, Aqmola and Pavlodar). P_JJA manifested an opposite trend to P_MAM across the entire country. SNOWc revealed negative anomalies over the northern and north-western (Aqtobe and Qostanay) part of Kazakhstan, with positive anomalies over central and north-eastern provinces (figure 1 and supplementary figure S1). T_{air} and LST exhibited a negative anomaly (decrease in temperature) over Kazakhstan's central portion, with a slight increase in temperatures over the other regions. SM and VOD exhibited similar trends, with a significant decrease in northern regions and a significant increase in other country regions (supplementary figure S1). TWS showed positive anomalies over northern and north-eastern parts of Kazakhstan, with significant negative anomalies over western and southwestern regions (Qyzylorda—figure 1 and supplementary figure S1).

Spatial trends of response and forcing variables

The MK test results for NDVI, NPP and ET revealed that the western provinces are experiencing decreasing trends in contrast to eastern provinces that have increasing trends. West Kazakhstan and Aqtobe provinces experienced a significant decrease

($p < 0.05$) in NDVI, NPP and ET, whereas East Kazakhstan and Almaty provinces experienced increased NPP (figure 4). NPP and ET had a magnitude ranging from -10 to 10 (g C m^{-2}/season and mm/season) across the country, whereas the magnitude of NDVI ranged from -0.03 to 0.03 (supplementary figure S2). P_MAM, P_JJA and VOD showed similar trends to NDVI, with decrease in West Kazakhstan, Mangghystau, Aqtobe, Almaty and Zhambyl provinces (figure 4). Spring precipitation had significant decreasing trends (magnitude <-5 mm/season) over the Pavlodar region and some portions of Aqtobe province. Summer precipitation had significant decreasing trends (magnitude <-5 mm/season) in West Kazakhstan, Aqtobe and some parts of South Kazakhstan, Zhambyl and Almaty provinces (figure 4 and supplementary figure S2). Though VOD had significant decreasing trends in West Kazakhstan, Aqmola, Pavlodar and some parts of Aqtobe, Qostanay, North and South Kazakhstan provinces, the magnitude of change was minimal across the country.

SNOWc exhibited significant increasing trends in West Kazakhstan and Atyrau regions. In contrast, there was decreasing trend in the central parts of Kazakhstan along with the mountainous regions of Almaty and East Kazakhstan provinces (figure 4). SM followed a similar trend to ET, with decrease in western provinces and in Zhambyl and Almaty provinces. Similar to VOD, SNOWc and SM had a minimal magnitude of change across the country (± 2%/season and ± 0.002, respectively; supplementary figure S2). T_{air} and LST showed similar trends in all provinces of Kazakhstan. A significant increase in temperature was found in western provinces along with a few provinces in southern parts of Kazakhstan. LST showed decreasing trends in North Kazakhstan and over the mountainous regions of Almaty and East Kazakhstan provinces (figure 4). T_{air} and LST had a magnitude of ± 0.1 degree/season across the country.

The MK trend for socioeconomic drivers showed that POP$_D$ had increased in most provinces except Qostanay, East and North Kazakhstan (table 2 and supplementary figure S3). The increasing and decreasing trends are significant ($p < 0.05$) for all provinces except Pavlodar. South Kazakhstan was experiencing the highest rate of increase (0.45 persons km^{-2} yr^{-1}), followed by Almaty and Aqmola (0.3 and 0.18 persons km^{-2} yr^{-1}, respectively) provinces (table 2). LSK$_D$ showed a significant increasing trend in all provinces of Kazakhstan, with a higher magnitude of increase in South Kazakhstan (1.48 heads/area of aimag/year), followed by Zhambyl and Almaty (0.51 and 0.45 heads/area of aimag/year) provinces. Mangghystau and Qyzylorda have a lower increase in magnitude and exhibited a non-significant trend ($p > 0.05$). GDPca showed a significant increasing trend in all provinces of Kazakhstan with a higher magnitude in Atyrau (1648.5 GDP per capita/year) followed by Mangghystau and Aqmola (791.42 and 685.95 GDP per capita/year) provinces (table 2 and supplementary figure S3). GDPca had a minimal increasing trend in South Kazakhstan and Zhambyl (188.08 and 193.52 GDP per capita/year) provinces, where LSK$_D$ was higher. CROPh showed significant trends in eight out of 14 provinces with a higher magnitude in Aqmola (0.009 tons ha^{-1} yr^{-1}), followed by South Kazakhstan and Qostanay (0.006 and 0.005 tons ha^{-1} yr^{-1}) provinces. Aqtobe and West Kazakhstan showed decreasing CROPh trends, whereas Atyrau and Almaty had higher significant increasing trends.

Precipitation and snow cover as latent variables (model 2–model 7)

In model-2 (supplementary figure S4(b)), P_MAM (SPC of 0.64) exhibited a strong positive influence on NDVI compared to summer precipitation—P_JJA (SPC of 0.29). P_JJA was removed from further SEM computations as it negatively impacted fit statistics (table 3, AIC from 4143 to 4667). Model-3 introduced VOD (WATRc LC) and showed that VOD improved the model fit and had a strong positive influence (SPC of 0.58) compared to other driving variables (supplementary figure S4(c), model-3, table 3). SM, introduced in model-4, showed a significant positive influence on NDVI in combination with VOD (supplementary figure S4(d)) that explained approximately 75% of the variability in NDVI (SPC of 0.75). The joint interaction of SM and VOD reduced all other predictor variable's impacts on NDVI, including the strong positive influence of P_MAM (SPC from 0.69 to 0.22). However, SM was removed from successive SEM models as it resulted in poor model fit statistics (table 3, AIC from 4143 to 4589).

TWS, introduced in model-5 (table 3, supplementary figure S4(e)), showed a significant positive influence on NDVI (SPC of 0.29). T_{air} and LST (Heat stress LC) added in models-6 and 7 (table 3, supplementary figures S4(f) and (g)) revealed a significant negative interaction with NDVI. The joint interaction of T_{air} and LST degraded the model fit (table 3, AIC from 4143 to 5326), so it was removed from further SEM analysis.

ORCID iDs

Kolluru Venkatesh ⦿ https://orcid.org/0000-0002-2110-5560
Ranjeet John ⦿ https://orcid.org/0000-0002-0150-8450
Jiquan Chen ⦿ https://orcid.org/0000-0003-0761-9458
Vincenzo Giannico ⦿ https://orcid.org/0000-0002-9907-3730

Sakshi Saraf ⦿ https://orcid.org/0000-0002-6785-8381

Maira Kussainova ⦿ https://orcid.org/0000-0002-9800-6093

References

A G, Velicogna I, Kimball J S and Kim Y 2015 Impact of changes in GRACE derived terrestrial water storage on vegetation growth in Eurasia *Environ. Res. Lett.* **10** 124024

Abel C, Horion S, Tagesson T, De Keersmaecker W, Seddon A W R, Abdi A M and Fensholt R 2021 The human–environment nexus and vegetation–rainfall sensitivity in tropical drylands *Nat. Sustain.* **4** 25–32

Andela N, Liu Y Y, van Dijk A I J M, de Jeu R A M and McVicar T R 2013 Global changes in dryland vegetation dynamics (1988–2008) assessed by satellite remote sensing: comparing a new passive microwave vegetation density record with reflective greenness data *Biogeosciences* **10** 6657–76

Apel H, Abdykerimova Z, Agalhanova M, Baimaganbetov A, Gavrilenko N, Gerlitz L, Kalashnikova O, Unger-Shayesteh K, Vorogushyn S and Gafurov A 2018 Statistical forecast of seasonal discharge in Central Asia using observational records: development of a generic linear modelling tool for operational water resource management *Hydrol. Earth Syst. Sci.* **22** 2225–54

Baydildina A, Akshinbay A, Bayetova M, Mkrytichyan L, Haliepesova A and Ataev D 2000 Agricultural policy reforms and food security in Kazakhstan and Turkmenistan *Food Policy* **25** 733–47

Beaudoing H and Rodell M (NASA/GSFC/HSL) 2020 GLDAS noah land surface model L4 monthly 0.25 × 0.25 degree V2.1 *Goddard Earth Sciences Data and Information Services Center (GES DISC)* (Greenbelt, MD) (https://doi.org/10.5067/SXAVCZFAQLNO)

Chen J *et al* 2015a Policy shifts influence the functional changes of the CNH systems on the Mongolian plateau *Environ. Res. Lett.* **10** 085003

Chen J *et al* 2015b Divergences of two coupled human and natural systems on the Mongolian plateau *Bioscience* **65** 559–70

Chen J *et al* 2021 Towards a single integrative metric on the dynamics of social-environmental systems *Sustainability* **13** 11246

Chen J *et al* 2022 Sustainability challenges for the social-environmental systems across the Asian Drylands Belt *Environ. Res. Lett.* **17** 023001

Chen Y, Li W, Deng H, Fang G and Li Z 2016 Changes in Central Asia's water tower: past, present and future *Sci. Rep.* **6** 35458

Chen Z, Wang W and Fu J 2020 Vegetation response to precipitation anomalies under different climatic and biogeographical conditions in China *Sci. Rep.* **10** 830

Dangal S R S, Tian H, Lu C, Pan S, Pederson N, Hessl A and Nippert J 2016 Synergistic effects of climate change and grazing on net primary production of Mongolian grasslands *Ecosphere* **7** 1–20

Dara A, Baumann M, Freitag M, Hölzel N, Hostert P, Kamp J, Müller D, Prishchepov A V and Kuemmerle T 2020 Annual Landsat time series reveal post-Soviet changes in grazing pressure *Remote Sens. Environ.* **239** 111667

de Beurs K M and Henebry G M 2004 Land surface phenology, climatic variation, and institutional change: analyzing agricultural land cover change in Kazakhstan *Remote Sens. Environ.* **89** 497–509

de Beurs K M, Henebry G M, Owsley B C and Sokolik I N 2018 Large scale climate oscillation impacts on temperature, precipitation and land surface phenology in Central Asia *Environ. Res. Lett.* **13** 065018

de Beurs K M, Henebry G M, Owsley B C and Sokolik I 2015 Using multiple remote sensing perspectives to identify and attribute land surface dynamics in Central Asia 2001–2013 *Remote Sens. Environ.* **170** 48–61

Deng Y *et al* 2020 Vegetation greening intensified soil drying in some semi-arid and arid areas of the world *Agric. For. Meteorol.* **292–293** 108103

Dong G, Zhao F, Chen J, Qu L, Jiang S, Chen J and Shao C 2021 Divergent forcing of water use efficiency from aridity in two meadows of the Mongolian plateau *J. Hydrol.* **593** 125799

Dong G, Zhao F, Chen J, Zhang Y, Qu L, Jiang S, Ochirbat B, Chen J, Xin X and Shao C 2020 Non-climatic component provoked substantial spatiotemporal changes of carbon and water use efficiency on the Mongolian plateau *Environ. Res. Lett.* **15** 095009

Dorigo W *et al* 2017 ESA CCI soil moisture for improved Earth system understanding: state-of-the art and future directions *Remote Sens. Environ.* **203** 185–215

Fan Y, Chen J, Shirkey G, John R, Wu S R, Park H and Shao C 2016 Applications of structural equation modeling (SEM) in ecological studies: an updated review *Ecol. Process.* **5** 19

Fernández-Giménez M E *et al* 2018 Using an integrated social-ecological analysis to detect effects of household herding practices on indicators of rangeland resilience in Mongolia *Environ. Res. Lett.* **13** 075010

Fetzel T, Havlik P, Herrero M and Erb K-H 2017 Seasonality constraints to livestock grazing intensity *Glob. Change Biol.* **23** 1636–47

Flammini A, Puri M, Pluschke L and Dubois O 2013 *Walking the Nexus Talk: Assessing the Water-Energy-Food Nexus in the Context of the Sustainable Energy for All Initiative* (available at: www.fao.org/3/a-i3959e.pdf)

Frühauf M, Meinel T and Schmidt G 2020 The Virgin Lands Campaign (1954–1963) until the breakdown of the Former Soviet Union (FSU): with special focus on Western Siberia *KULUNDA: Climate Smart Agriculture* (New York: Springer) pp 101–18

Giannico V, Spano G, Elia M, D'Este M, Sanesi G and Lafortezza R 2021 Green spaces, quality of life, and citizen perception in European cities *Environ. Res.* **196** 110922

Grace J B and Keeley J E 2006 A structural equation model analysis of postfire plant diversity in California shrublands *Ecol. Appl.* **16** 503–14

Grace J B, Schoolmaster D R, Guntenspergen G R, Little A M, Mitchell B R, Miller K M and Schweiger E W 2012 Guidelines for a graph-theoretic implementation of structural equation modeling *Ecosphere* **3** art73

Groisman P Y *et al* 2009 The Northern Eurasia Earth science partnership: an example of science applied to societal needs *Bull. Am. Meteorol. Soc.* **90** 671–88

Guo X, Chen R, Thomas D S G, Li Q, Xia Z and Pan Z 2021 Divergent processes and trends of desertification in Inner Mongolia and Mongolia *Land Degrad. Dev.* **32** 3684–97

Gutman G, Chen J, Henebry G M and Kappas M 2020 Landscape dynamics of drylands across Greater Central Asia: people, societies and ecosystems *Landsc. Ser.* **17** 1–236

Hall D K and Riggs G A 2016 MODIS/terra snow cover daily L3 global 500 m SIN grid, version 6 *NASA National Snow and Ice Data Center (NSIDC) Distributed Active Archive Center* (https://doi.org/10.5067/MODIS/MOD10A1.006)

Hankerson B R, Schierhorn F, Prishchepov A V, Dong C, Eisfelder C, Müller D and Forkuor G 2019 Modeling the spatial distribution of grazing intensity in Kazakhstan *PLoS One* **14** e0210051

Hao L, Pan C, Fang D, Zhang X, Zhou D, Liu P, Liu Y and Sun G 2018 Quantifying the effects of overgrazing on mountainous watershed vegetation dynamics under a changing climate *Sci. Total Environ.* **639** 1408–20

Hauck M, Artykbaeva G T, Zozulya T N and Dulamsuren C 2016 Pastoral livestock husbandry and rural livelihoods in the forest-steppe of east Kazakhstan *J. Arid Environ.* **133** 102–11

Hersbach H *et al* 2019 ERA5 monthly averaged data on single levels from 1979 to present *Copernicus Climate Change Service. Climate Data Store* (https://doi.org/10.24381/cds.f17050d7)

Hu Y, Han Y and Zhang Y 2020 Land desertification and its influencing factors in Kazakhstan *J. Arid Environ.* **180** 104203

John R *et al* 2016 Differentiating anthropogenic modification and precipitation-driven change on vegetation productivity on the Mongolian plateau *Landsc. Ecol.* **31** 547–66

John R, Chen J, Giannico V, Park H, Xiao J, Shirkey G, Ouyang Z, Shao C, Lafortezza R and Qi J 2018 Grassland canopy cover and aboveground biomass in Mongolia and Inner Mongolia: spatiotemporal estimates and controlling factors *Remote Sens. Environ.* **213** 34–48

John R, Chen J, Ou-Yang Z-T, Xiao J, Becker R, Samanta A, Ganguly S, Yuan W and Batkhishig O 2013 Vegetation response to extreme climate events on the Mongolian plateau from 2000 to 2010 *Environ. Res. Lett.* **8** 035033

Kim S J *et al* 2021 Developing spatial agricultural drought risk index with controllable geo-spatial indicators: a case study for South Korea and Kazakhstan *Int. J. Disaster Risk Reduct.* **54** 102056

Klein I, Gessner U and Kuenzer C 2012 Regional land cover mapping and change detection in Central Asia using MODIS time-series *Appl. Geogr.* **35** 219–34

Kong D, Zhang Q, Singh V P and Shi P 2017 Seasonal vegetation response to climate change in the Northern Hemisphere (1982–2013) *Glob. Planet. Change* **148** 1–8

Konkathi P and Karthikeyan L 2022 Error and uncertainty characterization of soil moisture and VOD retrievals obtained from L-band SMAP radiometer *Remote Sens. Environ.* **280** 113146

Kraemer R, Prishchepov A V, Müller D, Kuemmerle T, Radeloff V C, Dara A, Terekhov A and Frühauf M 2015 Long-term agricultural land-cover change and potential for cropland expansion in the former Virgin Lands area of Kazakhstan *Environ. Res. Lett.* **10** 054012

Kulmatov R 2014 Problems of sustainable use and management of water and land resources in Uzbekistan *J. Water Resour. Prot.* **06** 35–42

Lal R 2011 Sequestering carbon in soils of agro-ecosystems *Food Policy* **36** S33–S39

Landerer F W and Swenson S C 2012 Accuracy of scaled GRACE terrestrial water storage estimates *Water Resour. Res.* **48** 1–11

Li Y *et al* 2018 Divergent hydrological response to large-scale afforestation and vegetation greening in China *Sci. Adv.* **4** 1–10

Liang M, Chen J, Gornish E S, Bai X, Li Z and Liang C 2018 Grazing effect on grasslands escalated by abnormal precipitations in Inner Mongolia *Ecol. Evol.* **8** 8187–96

Liu P, Zha T, Jia X, Black T A, Jassal R S, Ma J, Bai Y and Wu Y 2019 Different effects of spring and summer droughts on ecosystem carbon and water exchanges in a semiarid shrubland ecosystem in Northwest China *Ecosystems* **22** 1869–85

Liu Y Y, Evans J P, McCabe M F, de Jeu R A M, van Dijk A I J M, Dolman A J, Saizen I and Chen H Y 2013 Changing climate and overgrazing are decimating Mongolian steppes *PLoS One* **8** e57599

Luo M, Liu T, Meng F, Duan Y, Bao A, Frankl A and De Maeyer P 2019 Spatiotemporal characteristics of future changes in precipitation and temperature in Central Asia *Int. J. Climatol.* **39** 1571–88

Mann H B 1945 Nonparametric tests against trend *Econom. J. Econom. Soc.* **13** 245–59

Meng E, Longmire J and Moldashev A 2000 Kazakhstan's wheat system: priorities, constraints, and future prospects *Food Policy* **25** 701–17

Meyfroidt P, Schierhorn F, Prishchepov A V, Müller D and Kuemmerle T 2016 Drivers, constraints and trade-offs associated with recultivating abandoned cropland in Russia, Ukraine and Kazakhstan *Glob. Environ. Change* **37** 1–15

Mirzabaev A, Ahmed M, Werner J, Pender J and Louhaichi M 2016 Rangelands of Central Asia: challenges and opportunities *J. Arid Land* **8** 93–108

Moesinger L, Dorigo W, de Jeu R, van der Schalie R, Scanlon T, Teubner I and Forkel M 2020 The global long-term microwave Vegetation Optical Depth Climate Archive (VODCA) *Earth Syst. Sci. Data* **12** 177–96

Nandintsetseg B, Shinoda M and Erdenetsetseg B 2018 Contributions of multiple climate hazards and overgrazing to the 2009/2010 winter disaster in Mongolia *Nat. Hazards* **92** 109–26

Petersky R S, Shoemaker K T, Weisberg P J and Harpold A A 2019 The sensitivity of snow ephemerality to warming climate across an arid to montane vegetation gradient *Ecohydrology* **12** 1–14

Prishchepov A V, Müller D, Dubinin M, Baumann M and Radeloff V C 2013 Determinants of agricultural land abandonment in post-Soviet European Russia *Land Use Policy* **30** 873–84

Qi J, Xin X, John R, Groisman P and Chen J 2017 Understanding livestock production and sustainability of grassland ecosystems in the Asian Dryland Belt *Ecol. Process.* **6** 22

Qiao D and Wang N 2019 Relationship between winter snow cover dynamics, climate and spring grassland vegetation phenology in Inner Mongolia, China *ISPRS Int. J. Geo-Inf.* **8** 42

Rolinski S, Prishchepov A V, Guggenberger G, Bischoff N, Kurganova I, Schierhorn F, Müller D and Müller C 2021 Dynamics of soil organic carbon in the steppes of Russia and Kazakhstan under past and future climate and land use *Reg. Environ. Change* **21** 73

Rosseel Y 2012 lavaan: an R package for structural equation modeling *J. Stat. Softw.* **48** 1–36

Sans P and Combris P 2015 World meat consumption patterns: an overview of the last fifty years (1961–2011) *Meat Sci.* **109** 106–11

Schierhorn F, Hofmann M, Adrian I, Bobojonov I and Müller D 2020 Spatially varying impacts of climate change on wheat and barley yields in Kazakhstan *J. Arid Environ.* **178** 104164

Sen P K 1968 Estimates of the regression coefficient based on Kendall's tau *J. Am. Stat. Assoc.* **63** 1379–89

Shi S, Yu J, Wang F, Wang P, Zhang Y and Jin K 2021 Quantitative contributions of climate change and human activities to vegetation changes over multiple time scales on the Loess Plateau *Sci. Total Environ.* **755** 142419

Shmelev S E, Salnikov V, Turulina G, Polyakova S, Tazhibayeva T, Schnitzler T and Shmeleva I A 2021 Climate change and food security: the impact of some key variables on wheat yield in Kazakhstan *Sustainability* **13** 8583

Solomon S, Plattner G-K, Knutti R and Friedlingstein P 2009 Irreversible climate change due to carbon dioxide emissions *Proc. Natl Acad. Sci.* **106** 1704–9

Suleimenov M and Oram P 2000 Trends in feed, livestock production, and rangelands during the transition period in three Central Asian countries *Food Policy* **25** 681–700

Sun Y-L, Shan M, Pei X-R, Zhang X-K and Yang Y-L 2020 Assessment of the impacts of climate change and human activities on vegetation cover change in the Haihe River basin, China *Phys. Chem. Earth* A/B/C **115** 102834

Swinnen J, Burkitbayeva S, Schierhorn F, Prishchepov A V and Müller D 2017 Production potential in the "bread baskets" of Eastern Europe and Central Asia *Glob. Food Secur.* **14** 38–53

Tian F *et al* 2018 Coupling of ecosystem-scale plant water storage and leaf phenology observed by satellite *Nat. Ecol. Evol.* **2** 1428–35

Tomaszewska M A and Henebry G M 2020 How much variation in land surface phenology can climate oscillation modes explain at the scale of mountain pastures in Kyrgyzstan? *Int. J. Appl. Earth Obs. Geoinf.* **87** 102053

Tomaszewska M A, Nguyen L H and Henebry G M 2020 Land surface phenology in the highland pastures of montane Central Asia: interactions with snow cover seasonality and terrain characteristics *Remote Sens. Environ.* **240** 111675

Ugbaje S and Bishop T 2020 Hydrological control of vegetation greenness dynamics in Africa: a multivariate analysis using

satellite observed soil moisture, terrestrial water storage and precipitation *Land* **9** 15

Venkatesh K, John R, Chen J, Xiao J, Amirkhiz R G, Giannico V and Kussainova M 2022 Optimal ranges of socio-environmental drivers and their impacts on vegetation dynamics in Kazakhstan *Sci. Total Environ.* **847** 157562

Wang W, Liang T, Huang X, Feng Q, Xie H, Liu X, Chen M and Wang X 2013 Early warning of snow-caused disasters in pastoral areas on the Tibetan Plateau *Nat. Hazards Earth Syst. Sci.* **13** 1411–25

Wang X, Wu C, Peng D, Gonsamo A and Liu Z 2018 Snow cover phenology affects alpine vegetation growth dynamics on the Tibetan Plateau: satellite observed evidence, impacts of different biomes, and climate drivers *Agric. For. Meteorol.* **256–257** 61–74

Wang Z, Deng X, Song W, Li Z and Chen J 2017 What is the main cause of grassland degradation? A case study of grassland ecosystem service in the middle-south Inner Mongolia *Catena* **150** 100–7

Wen Y *et al* 2019 Cumulative effects of climatic factors on terrestrial vegetation growth *J. Geophys. Res. Biogeosci.* **124** 789–806

Wright C K, de Beurs K M and Henebry G M 2012 Combined analysis of land cover change and NDVI trends in the Northern Eurasian grain belt *Front. Earth Sci.* **6** 177–87

Xi X and Sokolik I N 2016 Quantifying the anthropogenic dust emission from agricultural land use and desiccation of the Aral Sea in Central Asia *J. Geophys. Res. Atmos.* **121** 12270–81

Xie B, Jia X, Qin Z, Shen J and Chang Q 2016 Vegetation dynamics and climate change on the Loess Plateau, China: 1982–2011 *Reg. Environ. Change* **16** 1583–94

Xie X, He B, Guo L, Miao C and Zhang Y 2019 Detecting hotspots of interactions between vegetation greenness and terrestrial water storage using satellite observations *Remote Sens. Environ.* **231** 111259

Yan H, Lai C, Akshalov K, Qin Y, Hu Y and Zhen L 2020a Social institution changes and their ecological impacts in Kazakhstan over the past hundred years *Environ. Dev.* **34** 100531

Yan X, Li J, Shao Y, Hu Z, Yang Z, Yin S and Cui L 2020b Driving forces of grassland vegetation changes in Chen Barag Banner, Inner Mongolia *GISci. Remote Sens.* **57** 753–69

Yang Y, Wang Z, Li J, Gang C, Zhang Y, Zhang Y, Odeh I and Qi J 2016 Comparative assessment of grassland degradation dynamics in response to climate variation and human activities in China, Mongolia, Pakistan and Uzbekistan from 2000 to 2013 *J. Arid Environ.* **135** 164–72

Yuan J, Chen J, Sciusco P, Kolluru V, Saraf S, John R and Ochirbat B 2022 Land use hotspots of the two largest landlocked countries: Kazakhstan and Mongolia *Remote Sens.* **14** 1805

Zhang L, Xiao J, Li J, Wang K, Lei L and Guo H 2012 The 2010 spring drought reduced primary productivity in southwestern China *Environ. Res. Lett.* **7** 045706

Zhang Y, Wang Q, Wang Z, Yang Y and Li J 2020 Impact of human activities and climate change on the grassland dynamics under different regime policies in the Mongolian Plateau *Sci. Total Environ.* **698** 134304

Zheng K, Wei J-Z, Pei J-Y, Cheng H, Zhang X-L, Huang F-Q, Li F-M and Ye J-S 2019 Impacts of climate change and human activities on grassland vegetation variation in the Chinese Loess Plateau *Sci. Total Environ.* **660** 236–44

Zhou X, Yamaguchi Y and Arjasakusuma S 2018 Distinguishing the vegetation dynamics induced by anthropogenic factors using vegetation optical depth and AVHRR NDVI: a cross-border study on the Mongolian Plateau *Sci. Total Environ.* **616–617** 730–43

Zhou Y, Zhang L, Fensholt R, Wang K, Vitkovskaya I and Tian F 2015 Climate contributions to vegetation variations in Central Asian Drylands: pre- and post-USSR collapse *Remote Sens.* **7** 2449–70